

# **Sand Rate Model and Data Processing Method for Non-intrusive Ultrasonic Sand Monitoring in Flow Pipeline**

Guowang Gao<sup>1</sup>, Ruirong Dang<sup>1</sup>, Alireza Nouri<sup>2</sup>, Huiqin Jia<sup>1</sup>, Lipin Li<sup>1</sup>, Xudong Feng<sup>1</sup>, Bo Dang<sup>1</sup>

<sup>1</sup>School of Electronic Engineering, Xi'an Shiyou University, Xi'an Shaanxi, China, 710065.

<sup>2</sup>School of Mining and Petroleum Engineering, University of Alberta, Edmonton, Canada.

## **Abstract**

Sand production is a critical issue during oil and gas production from sandstone reservoirs. Uncontrolled sand production not only poses the risk of well failure, but also can cause extensive damage to surface and subsurface facilities such as tubing, pumps, valves and pipelines. In recent decades, research on sand production has been conducted in several fronts including sanding prediction, sand monitoring, sand control and wellbore integrity analysis to prevent or alleviate sand production and its consequences. This paper mainly focuses on acoustic sand monitoring which produces real-time information that can be used for maximizing the safe production of hydrocarbon.

We developed a new methodology for processing the acoustic signals based on the kinetic energy of sand particles in the pipeline. Further, we developed a procedure for identifying and filtering acoustic noise from unrelated events. We validated the proposed methodology for signal processing against experimental data. The results indicated that the de-noising algorithm could filter out the noise from the acoustic data and the model was effective for assessing the sand rate.

Key words: Sand production, Sand monitoring, Non-intrusive acoustic sand monitor, Wavelet threshold de-noising algorithm

## **1. Introduction**

The ability to continuously monitor sand in the flow is extremely useful to petroleum engineers. The information can be used for minimizing erosion damage to the production facilities, avoiding the wellbore collapse, preventing equipment (pipeline and valves) damage, predicting sand production trends, and providing timely information for sand management measures (Sampson et al., 2002). A number of different types of sand monitoring techniques are used in the oil and gas industry. The most common sand monitors include Electrical Resistance (ER) probes and acoustic sand monitors. The latter includes acoustic probes and non-intrusive acoustic sensors (Nabipour et al., 2012).

Electrical Resistance probes detect sand by means of monitoring the degree of erosion on a probe inserted in the flow stream. The probes are made from a thin metal film as the sensing elements. The thickness of the probe is reduced due to erosion by the sand particles in the flow stream. By measuring the electrical resistance of the sensing element over time, the amount of thickness reduction of the element can be determined. Empirical equations are used to relate the loss of element wall thickness to the amount of produced sand (Nabipour et al., 2012). This type of sand monitors is not used at low sand velocities or concentrations. Further, while the method can provide a reasonable assessment of the cumulative mass of sand production, it is not effective in providing the real-time or instantaneous indication of sand production (Brandal et al., 2010).

Ultrasonic sensor is another intrusive sensor that consists of a piezoelectric transducer and a thin-walled tube coated by titanium-carbide and filled with a light mineral oil. The probe responds to entrained solids and produces an output pulse signal. The output is proportional to the kinetic energy of the striking sand, which can be related to the solid concentration (Nabipour et al., 2012). The ultrasonic sensor works best at high flow velocities, which are usually found in gas wells. Their use is not recommended at velocities lower than 5 m/sec (Mullins et al., 1974).

Non-intrusive methods involve “listening” the sound generated by sand particles impacting the pipe wall (Allahar, 2003). Non-intrusive acoustic sensors are attached to the outside of a pipeline. To maximize signal detection, non-intrusive acoustic sensors should be installed about two-pipe diameter after pipe elbows (Haugen et al., 1995). Figure 1 shows the working principle and location of non-intrusive sand sensors. They can provide real-time sanding information and allow building an early warning system for any increased sanding activities (Nabipour et al., 2012). Non-intrusive acoustic sand monitors are also able to detect far lower sand concentrations than the intrusive types (Allahar, 2003).

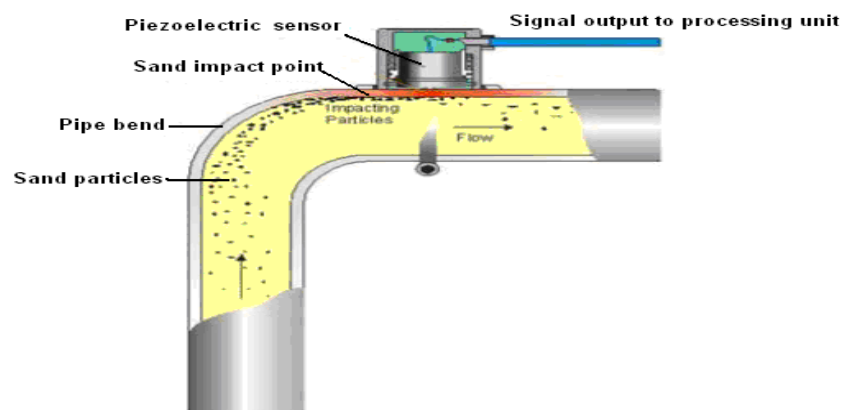


**Fig. 1 Passive non-intrusive ultrasonic sand sensor (Emiliani, 2011)**

In addition to the signals that are generated by the impact of sand particles on the pipeline wall, non-intrusive sand sensors also detect background noise that is produced by the flow turbulence, and the impact of gas bubbles or liquid droplets on the pipe wall (Shiraz, 2000). Additionally, the pre-processing circuit in the sand acoustic sensor and analog-to-digital conversion circuit can generate electrical noise. Generally, noise signals should be filtered before interpreting the ultrasonic signals.

Theoretically, any sand particles in the flow stream should produce an acoustic signal above the background noise level. The signal characteristics depend on various parameters such as the sand concentration in the flow stream, size and angularity of the sand particles, the velocities of sands impinging on the pipe wall, the fluid flow properties (flow regime, velocity, viscosity), and the pipe geometry (Allian, 2003). Equation (1) presents an existing formula for calculating the sand rate using the data from non-intrusive acoustic sensors (Ibrahim, 2008; Lazarus, 2005; Sampson et al., 2002):

$$SandRate = \left( \frac{Signal - Zero}{Step} \right)^{trend} \quad (1)$$

where *Signal* is the raw output from the sand sensor, *Zero* is the background noise, and *Step*

and *trend* are experimentally determined factors which are sensitive to the flow velocity, and sand particles size. The values of *Step* and *trend* are obtained from calibration work (Ibrahim, 2008).

The validity of Eq. (1) has been questioned because the calibration is related to the flow attributes and must be renewed as the flow conditions change (Oudeman, 1993). Further, the processed signal is not the output voltage of the piezoelectric crystal. Instead, it is the Root Mean Square (RMS) value of the crystal output. Another equation for calculating the sand mass rate was proposed by Sampson (2002):

$$\left(S_{pRMS}^2 - S_{bRMS}^2\right)^{\frac{1}{2}} = C\sqrt{m_t} \frac{1}{2}mv^2 \quad (2)$$

where  $S_{pRMS}$  is the RMS value of raw output,  $S_{bRMS}$  is the RMS value of background noise,  $m_t$  is the sanding mass rate,  $C$  is a calibration constant,  $m$  is the representative particle mass that can be found by calculating a representative particle diameter, assuming spherical particles and the density of the sand, and  $v$  is the representative particle impact velocity that is obtained from a multiphase erosion model (McLaury, 1993).

To use Eq. (2), the particle mass and velocity must be known. Although the method for finding the mass and velocity of sand particles has been specified, it is difficult to measure the accurate value for the size of sand particles and track the impact velocity of sand particles (McLaury, 1993). Therefore, to simplify the procedures for calculating the sand rate from Eq. (2), it has been assumed that all particles have the same mass and velocity. However, this assumption is not realistic rendering questionable results.

In this paper, we introduce a model that relaxes the assumptions of uniform sand grains and impact energy and considers the influence of the noise on the calculated sand rate. We have performed several laboratory tests to validate the proposed model.

## 2. New Model Derivation

The new model relates the sand rate to the acoustic signal generated by sand impacting the pipe wall. The assumptions used in the model formulation include:

(1) During the time of observation ( $\Delta t$ ), the in-situ volume rate of fluid flow ( $Q$ ) is constant and the velocity of solids in the pipe is  $v=Q/A$ , where  $A$  is the cross-sectional area of the pipe on which the sensor is installed.

(2) There is sufficient mixing of fluids and sand particles, which allows the assumptions of uniform sand concentration in the flowing fluid. Assuming all sand particles impact the pipe wall, the mass rate of sand particles passing the pipe elbow is defined as:

$$m_t = M / \Delta t \quad (3)$$

where  $M$  is the total mass of solids passing the pipe elbow during the observation time  $\Delta t$ .

(3) Let  $m_i$  be the mass of the  $i^{th}$  sand particle striking the pipe elbow, and  $n$  be the number of sand particles striking the pipe elbow during the observation time  $\Delta t$ . Depending on the number of sand particles impacting the pipe well, the mass rate of sand passing the elbow of the pipe is proportional to  $m_i$ :

$$\sum_{i=1}^n m_i / \Delta t = km_t \quad (4)$$

where  $k$  is a constant which may not be equal to unity as not all the sand mass in the pipe may produce signals and can be detected by the sand monitors.

(4) Assume all sand particles flow at the same velocity as the fluids flow and that all fluid phases flow at the same velocities. Therefore, statistically, the sum of individual sand masses times the square of their velocities can be replaced by:

$$km_t (Q / A)^2 = km_t v^2 = \sum_{i=1}^n m_i v_i^2 / \Delta t \quad (5)$$

where  $\sum_{i=1}^n m_i v_i^2$  represents kinetic energy of sand particles,  $v_i$  is the velocity of the  $i^{\text{th}}$  particle, and

$A$  is the cross-sectional area of the pipe where the monitoring is taking place. In reality, there could be slippage between different fluid phases and the sand may flow at velocities smaller than the fluid phases.

Sand sensors not only detect the acoustic signals generated by the solid particles that impact the pipe wall, but also detect noise signals from other sources. In addition, sand sensors and analog-to-digital conversion circuit also generate electric noise signals. Hence, there always is non-zero output from the sensor. When sand particles hit the pipe wall, they generate acoustic signals above the existing background noise level. Therefore, the actual amplitude of ultrasonic signals is equal to the amplitude of the raw signal ( $S_p$ ) from the sensor minus the amplitude of the background noise ( $S_b$ ). The actual amplitude is related to the effective time rate of the change of kinetic energy:

$$S_p - S_b = \frac{c}{2\Delta t} \sum_{i=1}^n m_i v_i^2 \quad (6)$$

where  $c$  is a constant of proportionality.

Combine Eq. (5) and (6) to relate  $S_p - S_b$  to the rate of sand production:

$$S_p - S_b = \frac{ck}{2} m_t v^2 = \frac{ck}{2} m_t \left( \frac{Q}{A} \right)^2 \quad (7)$$

Equation (7) can be rearranged as follows:

$$m_t = \frac{2(S_p - S_b)}{ckv^2} = \frac{S_p - S_b}{K \left( \frac{Q}{A} \right)^2} \quad (8)$$

where  $K = \frac{ck}{2}$  is a constant of proportionality.

The total sand mass for a time period is given as follows:

$$M = \int_{t_1}^{t_2} m_t dt = \frac{A^2}{KQ^2} \int_{t_1}^{t_2} (S_p - S_b) dt \quad (9)$$

Theoretically, any solids introduced into the flow stream should produce acoustic signal. In reality, the increase in signal is dependent on various parameters, such as the sand concentration in the flow stream, the size and angularity of the sand particles, the composition of the fluids in the flow stream, and the angle at which sand particles hit the pipe wall, among others. Another important factor is the sensitivity of acoustic sensors, which dictates the lower-bound signal amplitude they can pick up. Further, signal detection can be influenced by some factors, such as sand settling and build-up of deposits on the pipe wall, that prevent sand particles from striking the pipe wall. The signals can also be influenced by the interference from other noise sources such as hydrate crystals, liquid particles, opening and closing of valves, and the operation of pumps and compressors. These parameters can influence the accuracy of sand monitoring. Improving the accuracy of sanding assessments from sand monitoring measurements is critical for field industrial application.

### 3. Signal Characteristics and Processing Method

Sand production rate is obtained from the measurement of the acoustic signals generated by sand impacting the pipe wall. The sensor sends an analog electrical signal to an instrument that converts this analog signal into a digital signal. The digital signal is then converted into sanding rate in grams per second. These signals can be displayed and recorded. In addition to the recording, alarm levels can be established and set in relation to quick changes in the level of sand production.

#### 3.1 Signal Characteristics

The challenge for non-intrusive ultrasonic sand monitoring is to filter out the noise from various sources such as mechanical and flow related sources. It is usually considered that the frequencies generated by particle impacts are from 100 kHz to 500 kHz and are different than the frequencies of the noise generated by gas bubbles or liquid droplets striking the pipe wall (Brown, 2000). Normally the noise from non-sanding events possesses lower amplitude and lower frequency compared to the acoustic signals generated by the sand impacts (Nabipour et al., 2012).

#### 3.2 General De-noising Methods

It is very important for sand monitoring system to reduce the noise in the signal. In some monitors, separation of the noise from sand signals is carried out by considering only the amplitude of the recorded data (Nabipour et al., 2012). However, this method cannot ensure efficient separation of sand signals from the noise. Therefore, it is often recommended that the filtering of certain ranges of frequency in the detected signal be included in the filtering process (Nabipour et al., 2012).

In general, there are two methods for reducing the noise in the signal. One is to use band-pass filter in the hardware circuit to process the analog signal. For instance, the piezoelectric transducer in the acoustic sand sensor can be tuned to magnify the response for a specific frequency range while attenuating the response in the noise frequencies.

The second method is that the analog signal generated by the sand acoustic sensor be converted into digital signal and sent to the computer where the noise is processed and filtered by using signal processing algorithms. Understanding the characteristics of the signal is critical in selecting the effective signal-processing algorithm. For instance, the acoustic signal produced by sand impacting the pipe wall is considered to be random signal due to random sand impinging on the pipe wall (Geng, 2003).

Usually, we combine the hard filtering and the signal processing algorithms to improve the signal. The hard band-pass filter can nearly completely remove the noise within a certain frequency band. However, it introduces electrical noise from analog devices. The application of signal processing algorithms can attenuate the remaining noise after the analog signal is converted to the digital signal. The advantage of signal processing algorithms is that they do not generate any additional noise. It is convenient to enhance the performance of the processed signal by adjusting the parameters of the algorithm or even changing the algorithm. It should, however, be noted that signal processing algorithms need computation time that may affect the real-time performance of the system.

### **3.3 Selected De-noising Method**

In this paper, we use hard band-pass filter to remove the noise signal in the noise frequencies and then use wavelet transform de-noising algorithm to filter the electric noise. The algorithm is an adaptive filtering method and need not identify the statistical features of the signal. As such, it is an effective method to reducing the noise of transient random signals. The de-noising algorithm based on wavelet transform threshold filter can suppress most noise and fully preserve the relevant signals (Zhang, 2011). Wavelet threshold de-noising algorithm is performed in three stages (Zhang, 2012; Donoho, 1995):

- Wavelet decomposition: Wavelet decomposition of the raw signal is performed to decompose the signal into different scales with different levels of resolution by wavelet transform. After wavelet decomposition, the wavelet decomposition coefficients are obtained that consist of the wavelet coefficient of signal and the wavelet coefficient of noise, which are used for threshold processing. In this step, it is important to choose an appropriate wavelet and number of layers (N) for wavelet decomposition.
- Threshold processing for wavelet decomposition coefficient: An appropriate threshold is chosen to determine the wavelet decomposition coefficient of each layer from 1 to N. In this process, the wavelet coefficient of signal is preserved. However, the wavelet coefficient of noise is replaced by the difference between the current coefficient and the chosen threshold if the wavelet coefficient of noise is greater than the chosen threshold. Otherwise the coefficient is assigned “zero” value.
- Signal reconstruction: The processed coefficients are used to reconstruct back the noise-free signal in the time domain by wavelet inverse transform.

The above processes indicate that selecting an appropriate number of wavelet layers and appropriate threshold should be fully considered. The wavelet de-noising algorithm provides four threshold rule options (Zhang, 2012; Zhang, 2011; Suo, 2006): (1) Mini-maxi threshold rule that can generate a fixed threshold; (2) Fixed Threshold Rule (FTR) in which the threshold based on

mini-maxi rule is multiplied by a fixed coefficient  $\sqrt{\text{Log}_e M}$ , where  $M$  is the length of signal; (3)

Unbiased Estimation Threshold Rule (UETR) in which the threshold can be generated by calculating the risk values for each scale threshold and choosing a threshold that minimizes the risk value ; (4) Mixing Threshold Rule (MTR) in which a threshold can be chosen automatically from the FTR and UETR depending on the signal.

### 3.4 Performance of Wavelet Transform De-noising Method

To illustrate the de-noising performance of the algorithm, we performed simulation experiments in MATLAB. First, we generated synthetic signal with a known level of Signal to Noise Ratio (SNR), which is defined as:

$$SNR(dB) = 10 \log_{10} \left[ \sum_{n=0}^{N-1} \frac{s^2(n)}{(s(n) - \hat{s}(n))^2} \right] \quad (10)$$

where the original signal is denoted  $s(n)$  and the de-noised signal is denoted  $\hat{s}(n)$ . According to Eq. (10), higher SNR indicates better de-noising performance.

Figure 2 shows the synthetic signal with the SNR of 7.4420. In order to compare the performance of different de-noising algorithms, we processed the signal by both Fourier transform de-noising algorithm and wavelet transfer algorithm. The results of two algorithms are shown in Fig. 3 and 4, respectively. We selected the Symlets wavelet family (a typical wavelet function) with five decomposition layers and soft mixing threshold to process the simulated signals. From Fig. 2-4, we find that both algorithms can reduce the noise signals and improve the smoothness of the original signal.

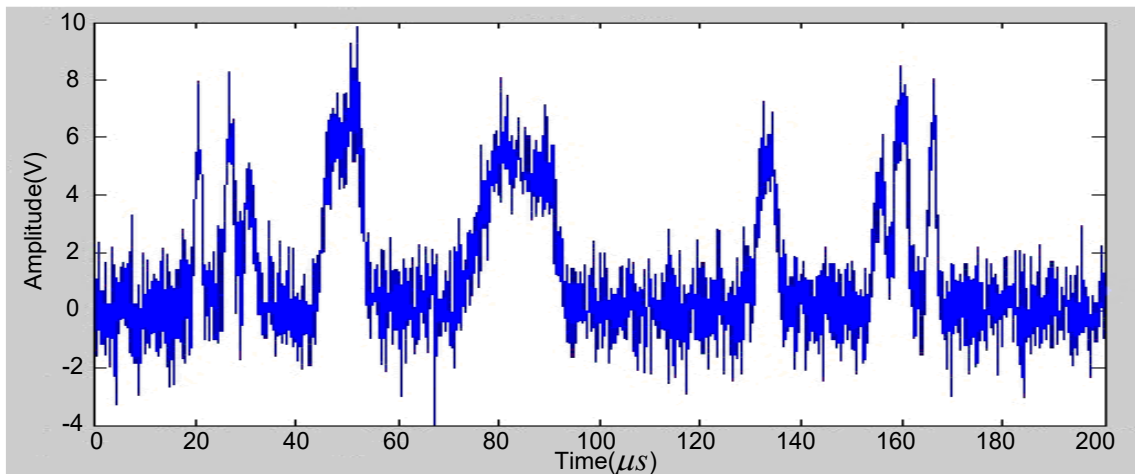
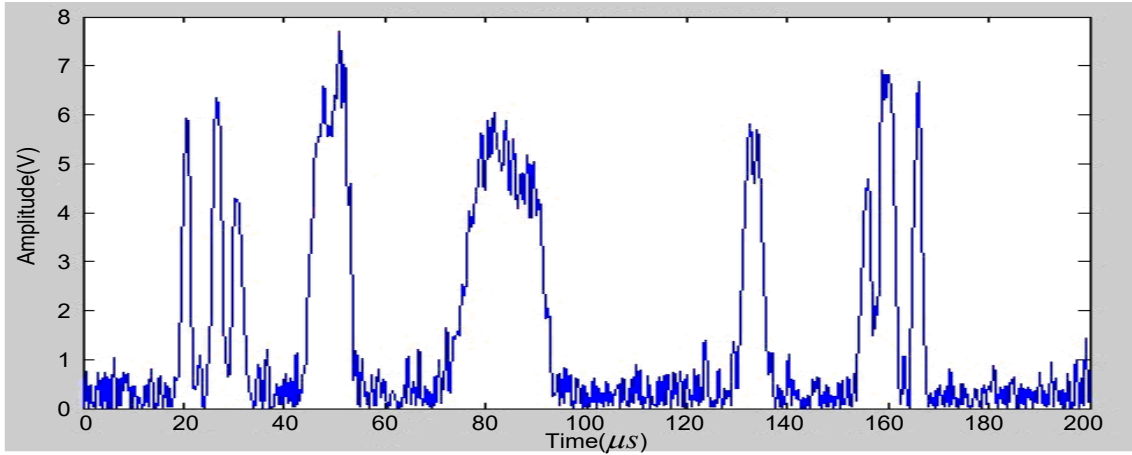
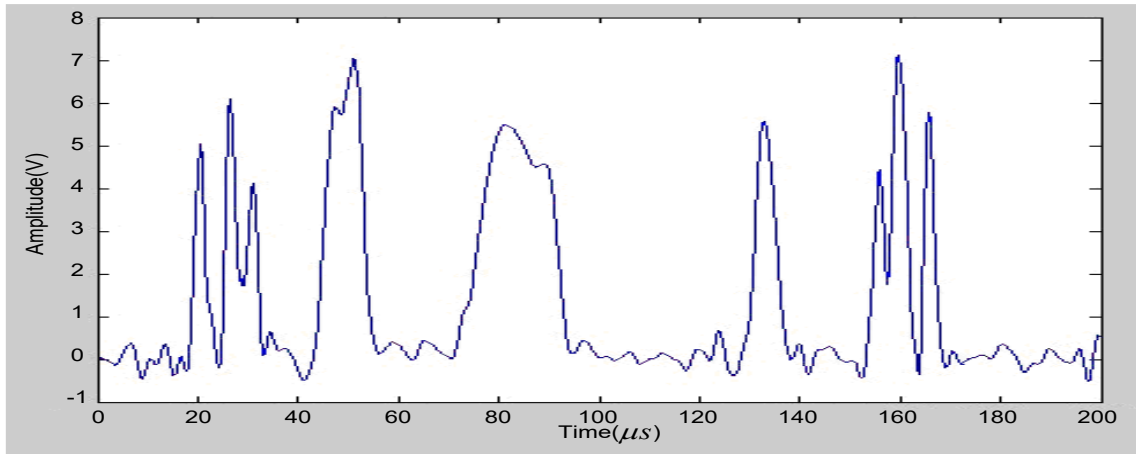


Fig. 2 Synthetic noisy signal



**Fig. 3 De-noised signal by FFT**



**Fig. 4 De-noised signal by the wavelet de-noising algorithm**

Next, the simulation signals with different SNR were processed. Table 1 shows the SNR results by the wavelet threshold de-noising algorithm and FFT de-noising algorithm. From the results of the two algorithms, we find: (a) the signal-noise ratio is improved when de-noising by the two methods; (b) SNR values (Table1) after de-noising show that the wavelet threshold de-noising algorithm is superior to the FFT algorithm in removing noise. Therefore, we determined that the wavelet threshold de-noising algorithm should be used to process the sand monitor signal.

**Table.1 De-noising results of the synthetic signal by two algorithms**

SNR of Synthetic Signals (dB)	SNR of de-noising by FFT (dB)	SNR of de-noising by Wavelet (dB)
1.4214	9.3614	14.1583
7.4420	15.4056	18.1244
10.9638	18.9556	21.5698
13.4626	21.4521	23.9697

To verify the performance of wavelet threshold de-noising algorithm under different number of decomposition layers and different threshold rules, we performed two sets of simulation experiments by using the artificial signals with SNR=7.440 and SNR=10.9638. In one, we calculated SNR after de-noising for different number of decomposition layers for the same wavelet

function and the same threshold (Fig.5). In the second simulation, we calculated SNR after de-noising for different thresholds using the same wavelet function and five decomposition layers. Figure 6 shows the results of the second simulation, which indicates: (1) For the same wavelet function and threshold rule, the performance of de-noising is improved with increasing the number of decomposition layers. However, the SNR result shows that the effect of de-noising is not improved beyond five decomposition layers. (2) For the same number of decomposition layers, the MTR is showing the best performance in this case. This type of analysis should be performed for every monitoring case in hand to determine the optimum algorithm and number of decomposition layers.

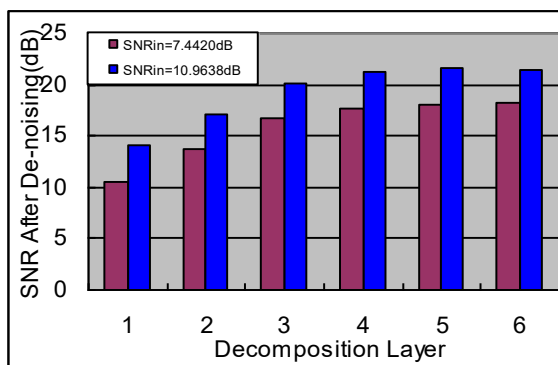


**Fig. 5** The de-noising results for different number of decomposition layers

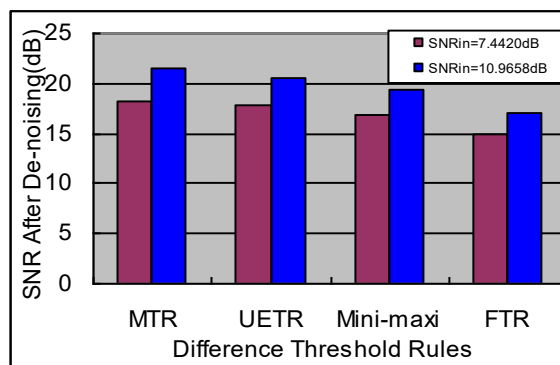


**Fig. 6** SNR for different de-noising threshold rules

We also tested the performance of signal processing algorithms on acoustic signals obtained from laboratory measurements. The SNR was still used to evaluate the performance of different de-noising algorithms. Figure 7 shows an original signal detected by ultrasonic sensor from laboratory testing that will be described later. Figure 8 shows the results of wavelet threshold de-noising algorithm with different number of decomposition layers and the MTR algorithm. Figure 9 shows the results of de-noising process using the wavelet threshold de-noising algorithm with different threshold rules and five decomposition layers. We chose two wavelet bases and compared the de-noising performance of each algorithm with different wavelet bases. The red curve indicates the results of Symlets wavelet base and the black curve indicates the results of Daubechies wavelet base. From the results of SNR, we find: (1) the number of decomposition layer affects the de-noising performance and the SNR value is nearly the same from four to six decomposition layers; (2) The MTR shows better performance than other three other threshold rules; (3) The two wavelet bases have nearly the same SNR for different decomposition layers, and the results of Symlets wavelet base is superior to that of Daubechies wavelet base for different threshold rules.

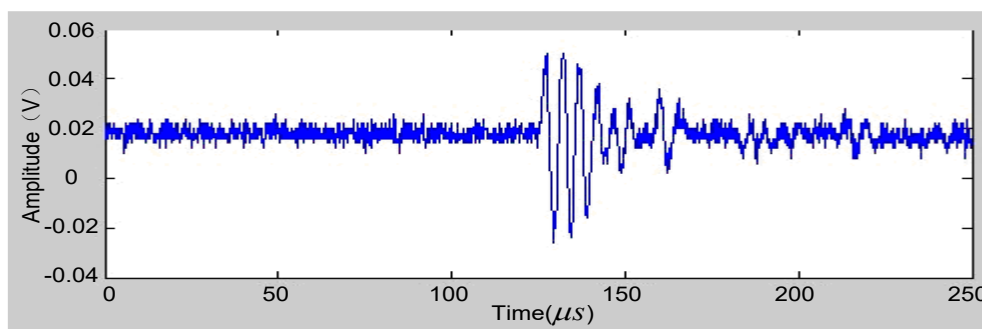


**Fig. 7 Signal from ultrasonic sensor measurements**

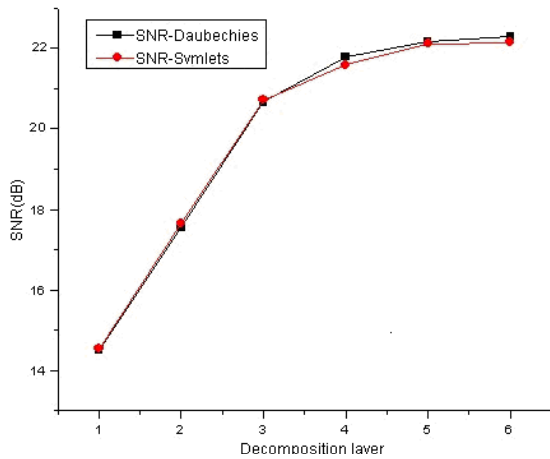


**Fig. 8 The SNR results of de-noised signal for different decomposition layers**

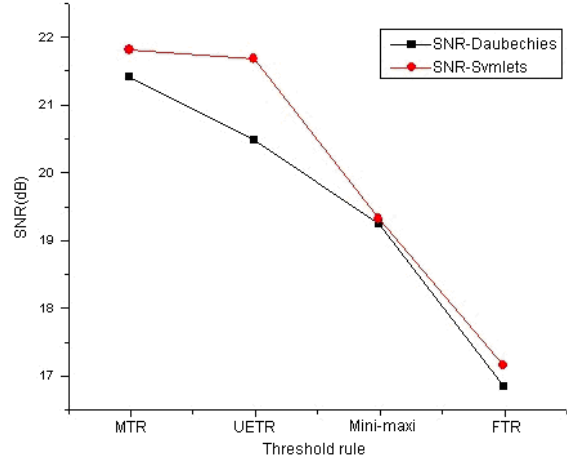
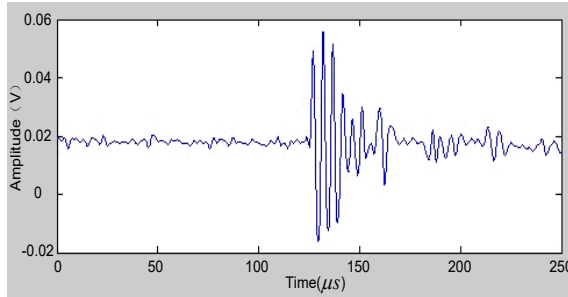
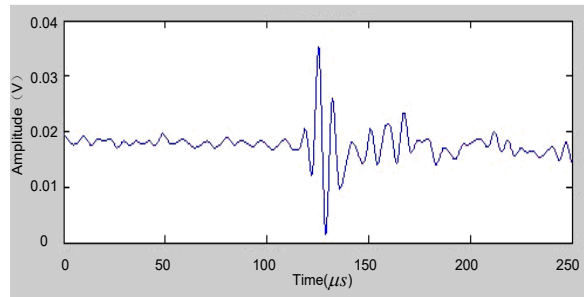


**Fig. 9 The SNR results of de-noised signal for different threshold rules**

De-noised signals using the MTR with four and five decomposition layers are shown in Fig. 10. The results indicate that the noise level is significantly reduced compared to the original signal. However, the de-noising result with five decomposition layers has lost amplitude for some events and is therefore not suitable for this case.



**(a) De-noising result with four decomposition layers**



**(b) De-noising result with five decomposition layers**

**Fig. 10 De-noising results with four and five decomposition layers**

#### 4. Sand Monitoring Software System

The sand monitoring system based on non-intrusive acoustic sensor consists of piezoelectric sensor, signal preprocessing board, and sand monitoring software, among others. The sand sensor can detect the signal generated by sand particles as well as the noise generated by, for instance, gas/liquid droplets impacting the pipe wall. The analog signal detected by the sand sensor is transmitted to the preprocessing circuits that may apply an initial filtering and amplify the remaining signals. The hard filtering is performed with the aim of preserving the signal generated by the sand impacts on the pipe wall and attenuating the noise signal. The amplifier circuit is designed to enhance the amplitude of the sand signal, which are then sent to the data acquisition system. The analog signal is then converted to digital signal by the data acquisition board with PCI interface. The sand monitoring software system can be designed within LabVIEW or similar platform and can handle the data acquisition, processing and display. The software system consists of five modules:

- The operator and well information module,

- The data acquisition module for which data acquisition frequency, acquisition length, and trigger type should be specified,
- The data processing module for sand rate calculations, wavelet filter algorithm, and frequency spectrum analysis,
- The display module, including the raw signal display, the processed signal display, frequency spectrum display, real-time sand rate and sand mass display,
- The data storage and recovery module for sand monitoring data, and petroleum production data for the analysis and prediction of sand production.

The sand monitoring interface with real-time data display is shown in Fig. 11.

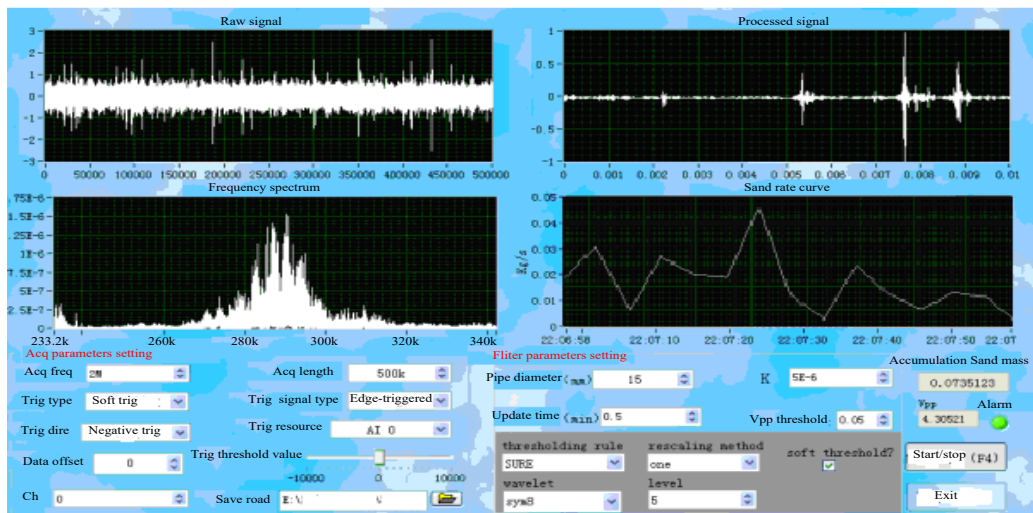


Fig.11 Sand monitoring display module

## 5. Laboratory Testing and Model Validation

We developed an experimental facility and a test procedure to simulate real-world sand flow as it occurs in petroleum production. The aim of experimental testing was to validate the sand rate model and the signal-processing algorithm against laboratory data.

### 5.1 The test rig

The test rig was designed by the sand monitoring research team and installed in Xi'an Shiyou University. The facility was designed to simulate multiphase flow and sand particle transportation in pipelines. Figure 12 shows the schematic design of the test rig and Fig. 13 presents an image of the test rig. The test rig is a closed loop, equipped with two fluid storage tanks, a gas compressor, and pumps for circulation of gas and liquid phases. In this rig, gas and liquid phases can be mixed and sand particles are injected into the mixture of the test loop section. The gas and fluid velocities can be measured independently. Pressure and temperature sensors are installed in the test loop. A certain amount of quartz sand is injected into the fluid flow, and the sand-monitoring sensor detects the signals produced by the sand particles hitting the pipe wall. The test rig includes a frequency conversion box that can adjust the motor rotating speed to control fluid flow velocity. In particular, the sand-monitoring sensor is mounted on the outer surface of a 1-in. diameter pipeline immediately downstream to a bent. In the test loop system, reducing the diameter of the pipe is necessary for increasing the kinetic energy of sand particles, hence, increasing the amount of signals detected by

the sand-monitoring sensor.

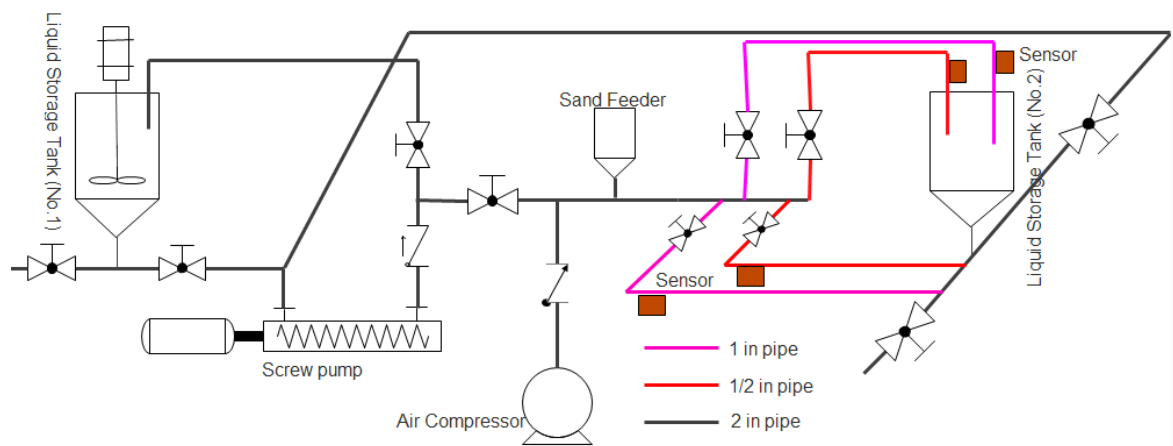


**Fig. 12 The test rig system design**



**Fig. 13 Image of the test rig in the laboratory**

## 5.2 Test Procedure and Results

A Coriolis mass flow meter was installed in the test rig and calibrated. Next, sand-monitoring system was tested to verify its performance. The test was first started by flowing water to record the system noise and identify the noise frequencies and amplitudes. Recorded data show that the frequencies of background noise and high frequency noise are outside of 100-500kHz. The flow rate was varied to obtain the noise characteristics for different flow velocities, and the amplitude of the noise was about 0.5V-1V with the different flow velocities from 5.0 m/s to 9.5 m/s. Fine sand (uniform grain size 100  $\mu$ m) was then injected into the pipe and the acoustic signals were detected. The total amount of injected sand was 3kg for each test, and the tests were repeated four times for each of the flow velocities of 5.5, 6.5, 7.5, and 8.5m/s.

The acoustic signals were first filtered by applying hard filtering and amplifying the amplitude of the remaining signals. Hard band-pass filtering was designed to attenuate the signal with frequencies outside of 100kHz to 500kHz. The processed signal and frequency spectrum could be recorded by a digital oscilloscope as shown in Fig. 14 and 15. The results show that the signals with the frequency range from 100kHz to 500kHz were enhanced but the signals outside of this

frequency range were attenuated.

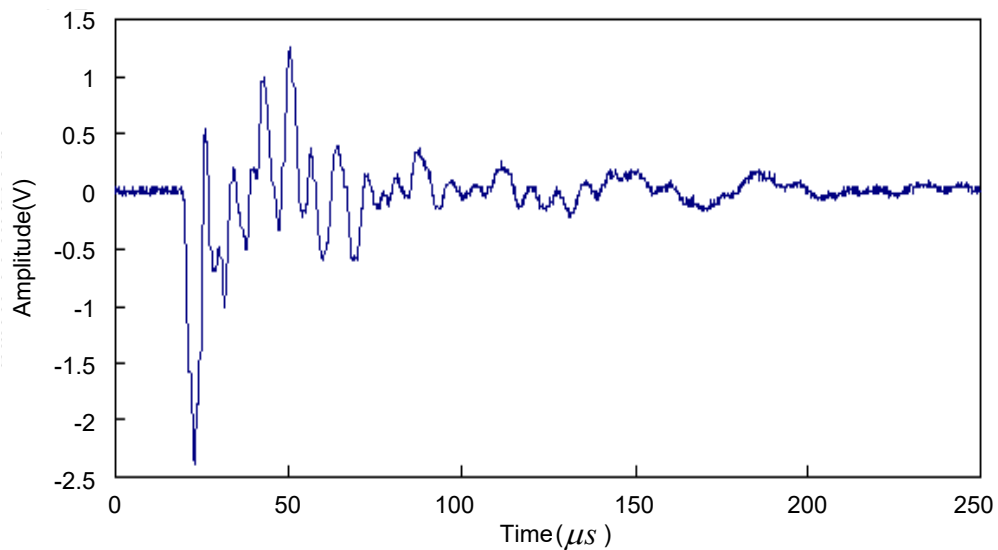


**Fig. 14 The processed signal by band-pass filtering**

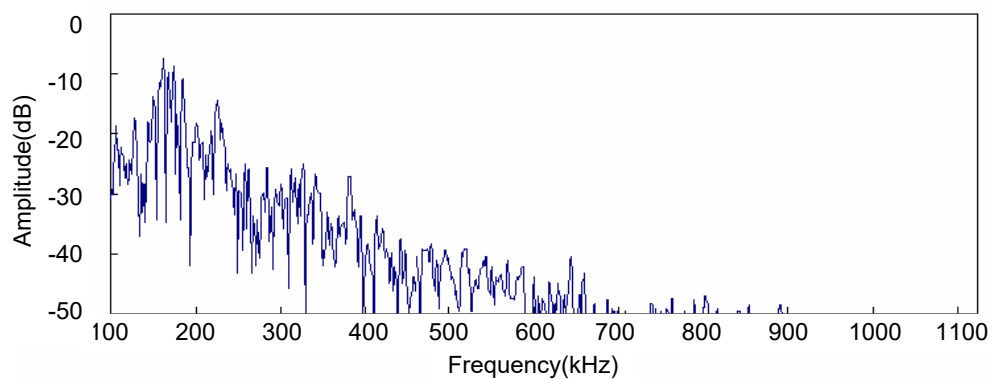


**Fig. 15 Frequency spectrum of the processed signal**

Next, analog signal were converted into digital signals, which were then transmitted to the computer. In the software for sand signal processing (see Fig.11), electric noise was filtered from the digital signals by wavelet threshold de-noising algorithm. Although the hard band-pass filtering is supposed to have removed the majority of the noise (see Fig. 14 and 15), the higher frequency electric noise from electrical devices is introduced to the digital signal, which need to be filtered. The wavelet threshold de-noising algorithm was used here to filter out the high-frequency electric noise. In the software interface, the wavelet base, threshold rule and the number of layers can be chosen and adjusted depending on the signal noise. Using the procedure described in previous sections, we chose the appropriate parameters (in this case, the Symlets wavelet base, MTR and five decomposition layers) to filter out the noise in the digital signal. Figure 11 shows the results that indicate improved SNR of the processed signal compared with that of the original signal.

Finally, the sand rate and accumulative amount of sanding were calculated by using Eq. 8-9. The model was calibrated for different flow velocities and different sand sizes. For each flow velocity and sand size, we performed the test four times to ensure reproducibility of the test results. Figure 16 and 17 present the results of cumulative sand production as assessed by Eq. 9 and compare the

assessment with the actual amount of injected sand. The horizontal axis in Fig. 16 and 17 represents the test number (from one to four).

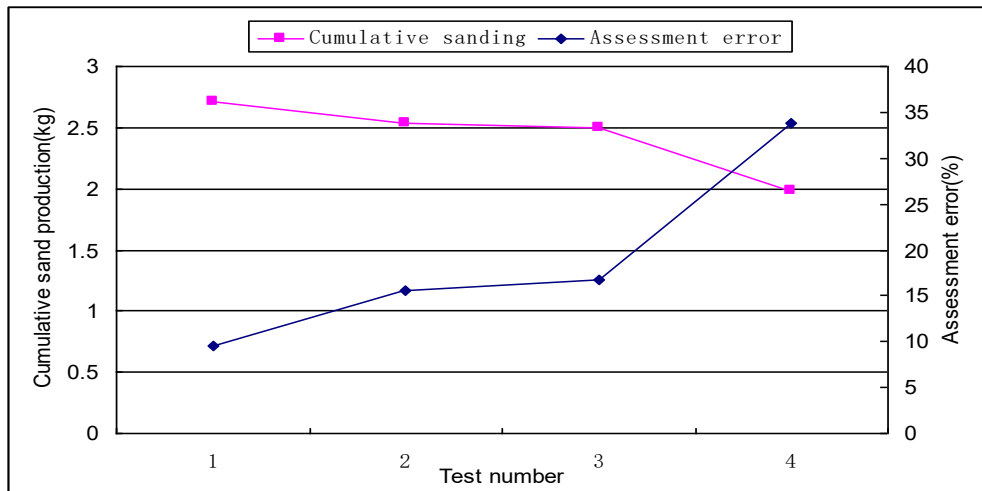


Fig. 16 Sand monitoring assessment at flow velocity 7.5m/s

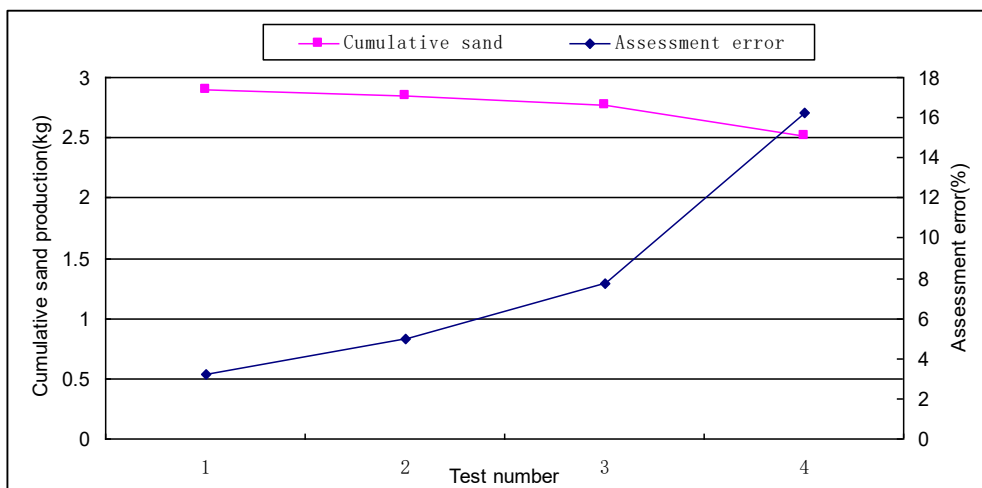


Fig. 17 Sand monitoring assessment at flow velocity 8.5m/s

The testing results indicate greater accuracy for the sand monitoring results for higher flow velocities. These laboratory tests allowed the validation of the proposed model and the signal-processing algorithm.

### 5.3 Laboratory Measurements Using Diluted Heavy Oil as the Medium

Sand production in heavy oil wells (e.g., in Steam Assisted Gravity Drainage wells) can be damaging. Therefore, it is beneficial to monitor sand production during heavy oil production.

We performed sand monitoring experiments using heavy oil from GuDong production plant in Shengli oilfield. The viscosity of this oil was higher than 30,000 mPa.s. Heavy oil viscosity reducer was used to reduce the viscosity to 220 mPa.s (35°C). Different flow velocities and different sand sizes were used in the testing.

In this testing, the sand monitoring system was the same as the testing with water flow. This includes the de-noising method, which was a combination of hard band-pass filtering and the

wavelet threshold de-noising algorithm, and the parameters of the processing algorithm, which were Symlets wavelet base, MTR and five decomposition layers.

The test was performed by injecting sand particles (sand diameter size: 100  $\mu\text{m}$ , mass: 500g) into the pipe. At flow velocities of less than 6.5 m/s, no signal was measured by the sand monitoring system. When the flow velocity was increased to 7.28 m/s, 163.9g was obtained by the sand monitoring system. At the flow velocity of 8 m/s, the error for sand rate assessment was above 40% compared to the actual amount of injected sand.

The test was then repeated for sand particle sizes of 100  $\mu\text{m}$  and 200  $\mu\text{m}$ , in which a total sand mass of 1000 g was injected into the pipe. At the flow velocity of 6.5m/s, the value of detected sand was only 153.7g. However, when the flow velocity was increased to 7.28 m/s, the amount of detected sand was increased to 772.5g indicating an error of 22.76%.

Next, the test was repeated with sand particle size of 500  $\mu\text{m}$  for a total injected sand mass of 500 grams at the flow velocity of 6.5m/s. The parameters of the whole system were held the same as the above testing In this case, the amount of detected sand was 411.4 grams.

Comparing the results of the sand monitoring between for the flow of water and diluted heavy oil, we can conclude that the fluid viscosity affects the accuracy of the sand monitor system. Further, it can be concluded that the accuracy depends on the sand particle diameter and the flow velocity as shown in Fig. 18.

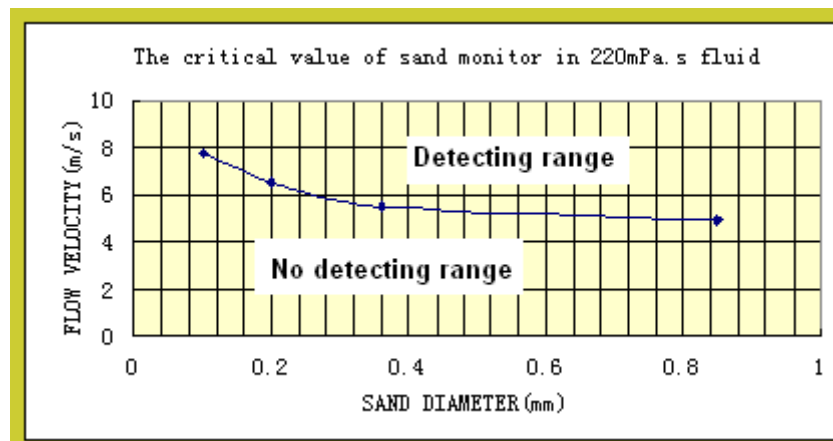


**Fig. 18** The relationship between the assessment error and the sand size and flow velocity

From the test results in the laboratory, we find that increasing the velocity of fluids at the measurement section is helpful to improve the accuracy of the measurements. Other factors, for instance the sensitivity of the sensor and the quality and methodology of signal processing are also important. We used passive ultrasonic sensors that were designed by our research team. The sensors consist of piezoelectric ceramic, sound wedge material and metal shell and their frequency response width are from 100kHz to 650kHz.

The de-noising process by hard band-pass filtering can inadvertently filter some signals generated by sand when their frequency falls outside of 100kHz to 500kHz affecting the accuracy of the sand rate assessments. It would be necessary to systematically investigate the frequency ranges of noise generated by different sources to minimize the removal of good data.

## 6. Conclusions

In the paper, a new model was developed for the sanding rate assessment from the signals detected by non-invasive acoustic sensors. A testing apparatus was also built to obtain the data for the calibration and validation of the proposed model.

Laboratory testing was performed by using water and the diluted heavy oil as fluid flow. We find that the viscosity of fluids, the velocities of fluids and particle sizes affect the accuracy of sand monitoring. In general, the higher the fluid velocity, the higher the accuracy is. For heavy oil, we found high flow velocities were needed (say greater than 6 m/sec for oil with viscosity of 200 mPas.sec) for the acoustic sensor to detect the sand in the flow. It appears this method is not suitable for sand detection in heavy oil flow unless the flow can be passed through a choke to increase the flow velocity immediately before a bent and the acoustic sensor.

The de-noising methods were investigated resulting in the choice of the combination of hard band-pass filtering for the analog signal and the wavelet threshold de-noising algorithm for the digital signal. The results of the simulation and testing show that the proposed de-noising method can improve the sand signal. In signal processing software, the parameters of wavelet threshold de-noising algorithm can be changed depending on the characteristics of the noise. For instance, the number of decomposition layers is often chosen from three to five layers for processing the sand signal.

The methodology can be used widely in the petroleum industry if the sand monitoring system is further optimized to improve the performance. The data processing software needs further improvement to reduce the assessment error for field operations.

## Acknowledgements

This research is funded by the Research Center of CNOOC and a consortium consisting of the Key Lab Research Funding of Shaanxi Province, the Key Discipline Funding on Instrument Science and Technology of Shaanxi Province, the Research Project Funding of Xi'an City, and the Doctoral Innovation Research Funding of Xi'an Shiyou University. The authors also thank Gudong Production Plant of SINOPEC Shenli Oilfield for providing heavy oil samples for use in laboratory testing.

## References

1. Sampson M., McLuary B., Shirazi S. 2002. A Method for Relating Acoustic Sand Monitor Output to Sand Rate and Particle Kinetic Energy, NACE International 2002, Houston, Texas, USA, NACE02248.
2. Nabipour A., Evans B., Sarmadivaleh, M., Kalli C. 2012. Methods for Measurement of Solid Particles in Hydrocarbon Flow Streams, SPE 158580. Presented at the SPE Asia Pacific Oil and Gas Conference and Exhibition, Perth, Australia, 22-24 October.
3. Brandal O., Wold K., Lilleland S.E., Hopkins S. 2010. The Development of Sand Monitoring Technologies and Establishing Effective, Control and Alarm-Based Sand Monitoring on a Norwegian Offshore Field, NACE International 2010, Houston, Texas, USA, Paper No.10142.
4. Shirazi S.A., McLuary B.S., Ali M.M. 2000. Sand Monitor Evaluation in Multiphase Flow, NACE International, 2000, Houston, Texas, USA, Paper No. 00084.
5. Mullins L.D., Baldwin W.F., Berry P.M. 1974. Surface Flow line Sand Detection,

SPE5152. Presented at the Second Midwest Oil and Gas Symposium of the Society of Petroleum Engineers of AIME, Indianapolis, Ind., March 28-29.

6. Brown G.K. 1997. External Acoustic Sensors and Instruments for the Detection of Sand in Oil and Gas Wells, the Offshore Technology Conference, Houston. Texas. 5-8 May 1997, OTC 8478.

7. Haugen S., Hodgson S., Upchurch J., McMahan J., Hazelrigg K., Mundorff J. 1995. Clamp on Ultrasonic Instruments in Subsea Applications, the 27th Annual Offshore Technology Conference, Houston, Texas, USA, 1-4 May 1995, OTC7746.

8. Allahar I.A. 2003. Acoustic Signal Analysis for Sand Detection in Wells with Changing Fluid Profiles, SPE 81002, Presented at the SPE Latin American and Caribbean Petroleum Engineering Conference, Port of Spain Trinidad, West Indies, 27-30 April.

9. Lazarus A. M., Temisanren T., Appah D. 2005. Establishing Actual Quantity of Sand Using an Ultrasonic Sand Detector, SPE 98820, Presented at the Niger Delta Experience, the 29th Annual SPE International Technical Conference and Exhibition, Abuja, Nigeria, 1-3 August.

10. Ibrahim, M., Haugsdal, T. 2008. Optimum Procedures for Calibrating Acoustic Sand Detector, Gas Field Case, the Canadian International Petroleum Conference/SPE Gas Technology Symposium 2008 Joint Conference, Calgary, Alberta, Canada, 17-19 June, Paper No. 2008-25.

11. Oudeman, P. 1992. Sand Transport and Deposition in Horizontal Multiphase Trunklines of Subsea Satellite Developments, SPE 25142, Presented at Offshore Technology Conference, Houston, U.S.A, 6-9 May.

12. Sampson, M. 2001. Determining a Relationship between Acoustic Sand Monitor Output , Particle Impact Energy and Sand Production Rate. M.S Thesis, Department of Mechanical Engineering. The University of Tulsa.

13. McLaury, B. 1993. A Model to Predict Solid Particle Erosion in Oilfield Geometries, M.S. Thesis, Department of Mechanical Engineering, The University of Tulsa.

14. Emiliani C.N., Lejon K., Linden M., Engene J., Kvernfold O., Packman C., Clarke D., Haugsdal, T. 2011. Improved Sand Management Strategy: Testing of Sand Monitors Under Controlled Conditions. SPE146679, Presented at the SPE Annual Technical Conference and Exhibition, Denver, Colorado, USA, 30 Oct-2 Nov.

15. Brown G.K., Davies J.R., Hamblde B.J. 2000. Solids and Sand Monitoring- An Overview, NACE International, 2000, Houston, Texas, NACE-00091.

16. Geng R., Li X., Pan X.. 2003. Dynamical Monitoring and Processing of Sanding Signals in Oil and Gas Wells. Computer Measurement & Control.11(9): 655-667.

17. Zhang W. 2011. Research on Detection and Treatment Technology of Oil Well Sand Production Signals, M.Sc. Thesis. School of Electrical Engineering, Xi'an Shiyou University, Xi'an China.

18. Wang F. 2009. Research and Application of Signal De-noising Based on Wavelet Analysis, M.Sc. Thesis. School of Electrical and Information Engineering University of Xihua, Chengdu, China.

19. Donoho D.L. 1995. De-noising by Soft-thresholding. *IEEE Trans on Information*, 41(3): 613-627.
20. Zhang Y., Zhou X, Guo Q. 2012 Wavelet Threshold De-noising Method of Ultrasonic Signal Based on LabView. *Computer Technology and Development*, 2012, 22(3): 125-128.
21. Suo J., Liang Z., Dong S., Huang C. 2006. Application of Wavelet Threshold De-noising Method in Processing Ultrasonic Signal, *Noise and Vibration Control*, 2006(3): 35-28.